

# Macromolecules

Volume 27, Number 9

April 25, 1994

© Copyright 1994 by the American Chemical Society

## Isotropic to Anisotropic Phase Transition of Extremely Long DNA in an Aqueous Saline Solution

Kunal Merchant and Randolph L. Rill\*

Department of Chemistry and Institute of Molecular Biophysics, The Florida State University, Tallahassee, Florida 32306-3006

Received August 13, 1993; Revised Manuscript Received December 28, 1993\*

**ABSTRACT:** The transition of simple aqueous saline solutions (buffered 0.1 M NaCl) of extremely long DNA (8 kilobases  $\approx 2.7 \mu\text{m} \approx 54$  persistence lengths) from the isotropic to anisotropic phase was characterized by solid-state  $^{31}\text{P}$  NMR spectroscopy and polarized light microscopy. The anisotropic phase first appeared in equilibrium with the isotropic phase at a concentration  $C_i^* = 13 \text{ mg/mL}$  and the isotropic phase disappeared at a concentration  $C_a^* = 67 \text{ mg/mL}$ . The first critical concentration ( $C_i^*$ ) is much lower than that observed for a stiffer polyelectrolyte (xanthan) and predicted by theory incorporating the influences of chain flexibility and charge. By contrast,  $C_a^*$  is in reasonable accord with expectations based on the static DNA persistence length ( $\approx 50 \text{ nm}$ ) in dilute solution. Since the dominant length scale for phase transitions of semiflexible polymers is the persistence length and not the contour length, this unexpected broadening of the biphasic region may reflect local, sequence-dependent variations in DNA flexibility.

### Introduction

In the past 4 decades theories of lyotropic liquid crystal formation by macromolecules have evolved from rudimentary descriptions of phase transitions of idealized models to encompass the behaviors of real semiflexible polymers. Onsager<sup>1</sup> in 1949 first predicted the formation of anisotropic phases in solutions of idealized long, thin, cylindrical rods based on considerations of the second virial coefficient in crowded isotropic and anisotropic solutions. Recently this approach has been extended by including the effects of charge<sup>2</sup> and flexibility.<sup>3,4</sup> In all cases formation of an anisotropic phase in equilibrium with the isotropic phase is predicted above a critical concentration  $C_i^*$  and a fully liquid crystalline phase above another critical concentration  $C_a^*$ . Both critical concentrations decrease with increasing polymer length, approaching an asymptotic limit at high axial ratios. For a given axial ratio the critical concentrations are expected to increase significantly with increasing chain flexibility as reflected by the persistence length.<sup>3,4</sup>

Behaviors qualitatively in agreement with theory have been observed for numerous nonelectrolyte polymers in organic solvents.<sup>5-7</sup> Critical concentrations determined in recent studies of carefully fractionated samples were in good quantitative agreement with theory incorporating effects of chain flexibility in nonelectrolytes<sup>5-8</sup> and flex-

ibility plus charge for a stiff, moderately strong polyelectrolyte (xanthan<sup>9,10</sup>).

Double-stranded DNA is a strong polyelectrolyte that is semirigid but possesses a higher charge density and greater flexibility than xanthan. A cholesteric DNA phase was first described by Robinson.<sup>11</sup> Various properties of anisotropic (principally cholesteric) phases of DNA were subsequently described in several other studies.<sup>12-30</sup> The ability to biochemically manipulate DNA offers practical advantages in preparing samples of defined length. Previously Rill and co-workers prepared and characterized phases formed by DNA fragments with a short, well-defined length ( $\approx 500 \text{ \AA}$ ) isolated from nucleosome core particles by enzymic digestion of chromatin.<sup>31-36</sup> Critical concentrations were determined for the isotropic to anisotropic phase transition, and the microscopic textures of three distinct phases ("precholesteric", cholesteric, and columnar) were reported.

Here we describe the first studies of phase transitions of exceptionally long DNA (median length  $\approx 8$  kilobases  $\approx 2700 \text{ nm}$ ,  $\text{MW} \approx 5 \times 10^6 \text{ D}$ ). Critical concentrations for anisotropic phase formation were determined by solid-state  $^{31}\text{P}$  NMR spectroscopy, and morphologies of anisotropic phases were examined by polarized light microscopy. The critical concentration,  $C_i^*$ , for the appearance of the anisotropic phase was only  $13 \text{ mg/mL}$ , much lower than that predicted based on the flexibility as expressed by the consensus static DNA persistence length in dilute solution. The birefringent "textures" of moderately concentrated,

\* Author to whom correspondence should be addressed.

• Abstract published in *Advance ACS Abstracts*, March 15, 1994.

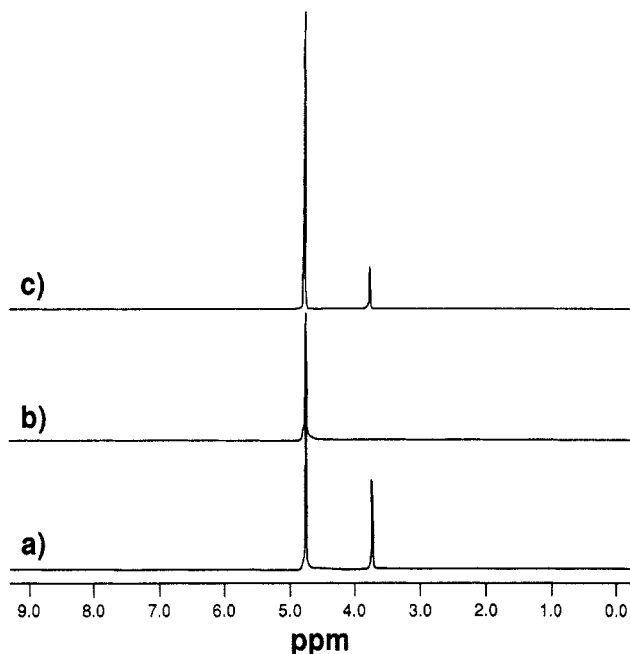


**Figure 1.** Proton ( $^1\text{H}$ ) NMR spectra of: (a) 6% PEG 6000 in  $\text{D}_2\text{O}$  (16 scans); (b) 10 mg/mL of DNA in  $\text{D}_2\text{O}$  (1036 scans); (c) same DNA as in b with PEG 6000 added to a final concentration of 0.6% (16 scans). Note that PEG resonances were readily observed in c, but no traces of PEG were observed in sample b subsequently used for studies of DNA phase transitions, despite greater signal averaging. Spectra were obtained at 270 MHz at room temperature. The resonance at 4.8 ppm is HOD.

biphasic solutions were poorly developed, in contrast to clearly cholesteric textures observed for low- and moderate-length DNA.<sup>15,36</sup>

Anisotropic phases of high molecular weight DNA not only provide information regarding the behavior of very long polyelectrolytes but also yield insights into DNA organization in living systems, which require orderly packing of very long DNA into small regions. The critical concentration for long DNA is well within the physiological concentration range of eukaryotic nuclei or bacterial nucleoids and far below concentrations of more tightly packaged DNA, e.g., in sperm heads or viruses. The tendency of DNA to self-order at physiological concentrations must therefore be included in any fundamental considerations of DNA packing *in vivo*.

## Experimental Section

**DNA Preparation and Characterization.** Highly polymerized calf thymus DNA was obtained from Sigma (Type I). This DNA was further purified by treating with RNase A, Proteinase K, and phenol-chloroform extraction,<sup>33</sup> using care to minimize shearing forces. (Purification was essential to remove considerable amounts of residual protein in the commercial preparation.) The highest molecular weight component of the purified DNA was precipitated with 6% PEG 6000.<sup>37</sup> PEG was removed by repeated precipitation from 70% ethanol. The elimination of PEG was confirmed by proton NMR (Figure 1). The size distribution of the DNA was determined by electrophoresis on a 0.6% agarose gel. Fragments of phage lambda DNA cleaved with the restriction endonuclease Hind III served as length markers. Gels were stained with ethidium bromide and photographed under 365-nm illumination using a Polaroid MP3 camera with Type 665 positive/negative film. Negatives were scanned with a BioRad Model 620 videodensitometer. Marker mobilities were used to compute a length distribution curve for the sample DNA. A plot of percent total area versus DNA size indicated that essentially all of the DNA was >1 kilobase pairs (kb), 80% was at least 4 kb long, 70% was between 4 and 13 kb, and the median length was  $\approx 8$  kb (Figure 2).

DNA samples for phase transition studies were dissolved in buffered sodium chloride (0.1 M NaCl, 10 mM Na cacodylate,

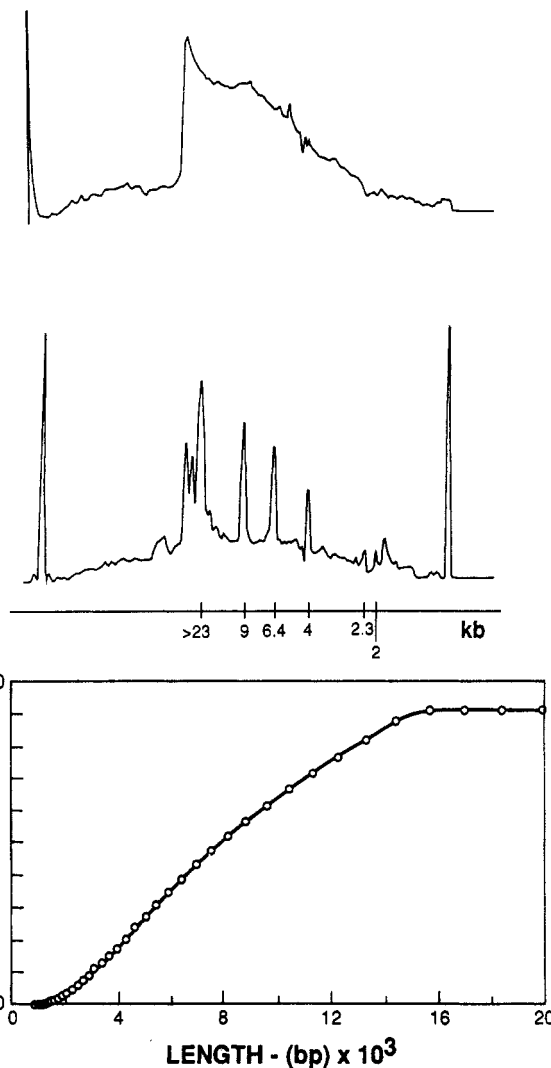


**Figure 2.** (Top) Densitometer scans of (a) the high molecular weight DNA electrophoresed on a 0.6% agarose gel and (b) Phage lambda DNA cut with the restriction endonuclease Hind III and electrophoresed beside the sample in a. Fragment lengths in kilobase pairs (kb) are indicated. (Bottom) Integral weight distribution of DNA lengths obtained by numerical integration of the densitometer scan in a calibrated using the DNA fragments in b.

5 mM EDTA, pH 6.5). A few concentrated solutions were prepared by centrifugal ultrafiltration using a Centriprep(R) filtration device (Amicon Inc.). Other samples were prepared by dilution of these samples after NMR measurements were completed and aliquots were withdrawn for microscopy and concentration determinations. Because of their extreme viscosities, samples were allowed to equilibrate over a period of at least a week at room temperature with occasional heating to 60 °C for 1–2 h before measurements were taken. Several spectra were recorded on each sample at intervals of 1 or more days until no changes were observed. In addition, several samples were examined 1–2 months after the initial series of experiments was completed. In all cases the fractional anisotropy was unchanged by the additional long equilibration time. At least three concentration measurements for each sample were made using an aliquot drawn by a positive displacement micropipette and were found to be within  $\pm 0.5$  mg/mL.

**NMR Spectroscopy.** Phosphorus-31 NMR spectra were taken on a nonspinning sample at a frequency of 109 Hz. The sweepwidth was  $\pm 8$  kHz, and a pulse repetition time of 20 s was used with gated proton decoupling during acquisition. Typically, 1000 scans were acquired for each data set. DNA samples were placed in 1.5-mL cylindrical tubes, cut so that 400  $\mu\text{L}$  of solution filled them without creating air bubbles. Because of sample heterogeneity, the sample tube was placed horizontally in a specially constructed coil and was totally enclosed by the coil. Spectra were deconvoluted using the program PEAKFIT (for

MS-DOS, Jandel Scientific) to fit to two components, a broad Gaussian resonance of anisotropic DNA and a sharper Lorentzian of isotropic DNA. The choices of these line shapes were dictated by the line shapes observed for the respective pure phases. Previous studies have shown that the breadth of the Gaussian resonance of the anisotropic phase of short DNA is mainly due to homogeneous broadening.<sup>38</sup> The fractions of total area under each of the curves determined the fractions of molecules in the respective phases.

The goodness of fit was indicated by the 99% confidence intervals, which were between 0.5% and 3% of the fitted curve, and the coefficients of determination ( $r^2$ ),<sup>39</sup> which were between 0.99 and 1. Very small amounts of isotropic or anisotropic phase are difficult to detect by NMR methods. The latter measurements are particularly sensitive to inadequate shimming or phasing. Spectra obtained under these conditions did not yield good fits to two components as described above and in such cases were reprocessed or reacquired. In addition, the fits obtained for the lowest concentration samples were strongly influenced by high-frequency noise in the broad, low-intensity "wings" of the Gaussian component. Attempts by the program to minimize errors in these wings led to nonsystematic exaggeration of the Gaussian component. Since the frequency of this noise was much greater than the intrinsic line width of the resonance of interest, a Fourier filtering technique within PEAKFIT (corresponding to truncation of the FID by 10%) was used to moderately smooth all spectra. Smoothing yielded fits that were significantly improved with respect to the above goodness of fit criteria, as well as the magnitude and randomness of the residuals. Analyses of smoothed spectra yielded consistent trends of decreasing Gaussian component with decreasing total DNA concentration that were qualitatively consistent with the microscopic appearances of the samples.

**Microscopy.** DNA solutions were observed between cross polarizers with a polarized light microscope (Nikon Microphot PolFX/A). Typically 20–30  $\mu$ L were placed on a microscope slide and a glass coverslip was sealed in place over it, using "Cytoseal Liquid Coverslip" (Stephens Scientific) on the edge. Slides were left to equilibrate overnight and then viewed. The samples with the highest DNA concentrations were viscous and translucent and did not spread on the slide very easily; therefore, they could not be sealed under a coverslip. Such samples were viewed and photographed immediately.

## Results

**<sup>31</sup>P NMR Spectroscopy.** As observed for short DNA, NMR spectra of biphasic solutions were characterized by two superimposed <sup>31</sup>P resonances, a broad Gaussian of the anisotropic phase and a sharper Lorentzian of the isotropic phase. Both resonances were broader than those observed for nucleosome length DNA (500 Å, 146 bp), as expected due to the greater length and higher solution viscosities. The width at half-maximum of the Lorentzian typically was 700–900 Hz, and that of the Gaussian varied from 1600 to 3000 Hz, increasing with increasing DNA concentration. A very close correspondence between the chemical shifts of isotropic and anisotropic resonances indicated that little alignment of the anisotropic phase occurred in the magnetic field, in contrast to the strong magnetic field alignment observed for anisotropic samples of short DNA.<sup>33,36</sup>

The area under each peak, after deconvolution, indicates the fraction of molecules in the isotropic ( $F_i$ ) and anisotropic phase ( $F_a$ ) at a total DNA concentration,  $C_D$ . Data were plotted as  $C_DF_a$  versus  $C_D$ , according to equation:

$$C_DF_a = \frac{C_a^*C_D}{C_a^* - C_i^*} - \frac{C_i^*C_a^*}{C_a^* - C_i^*} \quad (1)$$

as derived earlier,<sup>34</sup> where  $C_D$  is the total DNA concentration in mg/mL. (We note here an error in the sign of the first term of this equation in previous publications,<sup>34,40</sup>

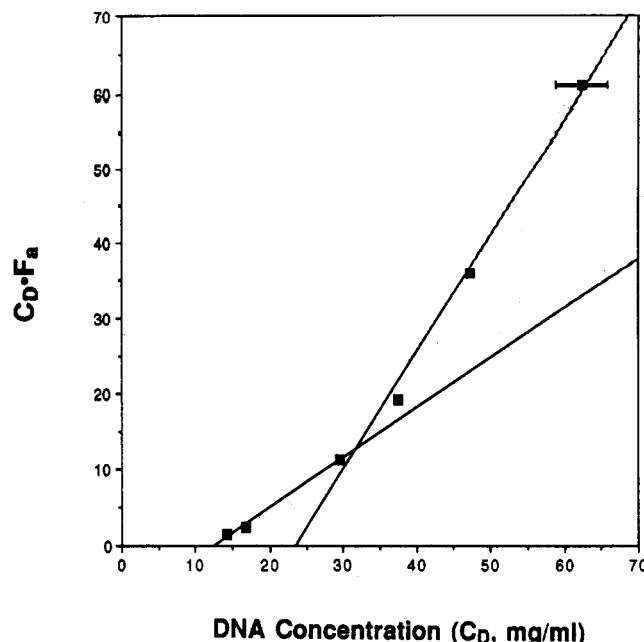


**Figure 3.** Total DNA concentration multiplied by the fraction of molecules in the anisotropic phase ( $C_DF_a$ ) versus the DNA concentration ( $C_D$ ) in mg/mL. The data point at 29 mg/mL was used to fit both straight lines. Extrapolation of these curves to 0% and 100% anisotropy yielded critical concentrations of  $C_i^* = 13$  mg/mL and  $C_a^* = 67$  mg/mL.

which is evident from the positive, not negative slope.) Extrapolations to the extremes yielded the critical concentrations for the appearance of the anisotropic phase,  $C_i^*$ , and the disappearance of the isotropic phase,  $C_a^*$ . In the present case this plot was not linear (Figure 3). Nonlinearity is perhaps not surprising since eq 1 is derived for the ideal case of a polymer of homogeneous length and flexibility (hence, homogeneous phase transition) and a single phase transition. Linear extrapolation of the low concentration region of the curve yielded a lowest estimate of  $C_i^* = 13$  mg/mL, while extrapolation excluding the two lowest concentration points yielded a higher estimate of  $C_i^* = 24$  mg/mL. The anisotropic phase disappeared at  $C_a^* = 67$  mg/mL.

The nonlinearity observed at low concentration could be due to heterogeneity of DNA length or flexibility. Incipient formation of a columnar phase at the higher DNA concentrations examined might also cause deviations from linearity. The origins of this phenomenon are not explored in detail here since the limiting values of  $C_i^*$  and  $C_a^*$  for long DNA chains are of primary concern.

**Polarized Light Microscopy.** The presence of the anisotropic phase in the lowest concentration (<20 mg/mL) solutions was confirmed by the observation of weak, unstructured birefringence (Figure 4A). No birefringence was observed for a 10 mg/mL sample, further supporting the NMR observations. Both techniques indicate that this limit is near the limit of 13 mg/mL extrapolated from NMR data.

The myriad of well-developed textures observed for anisotropic phases of shorter DNA was not observed for the high molecular weight DNA.<sup>36</sup> In particular, distinct spherulites or "globules" were not observed in weakly birefringent samples, and it was difficult to detect the "fingerprint" pattern characteristic of cholesteric phases in more concentrated samples, even after placement overnight in a high magnetic field. An increase in the background birefringence was noted with increasing concentration, and a change in texture was noted coincident with a change in the slope of the phase transition

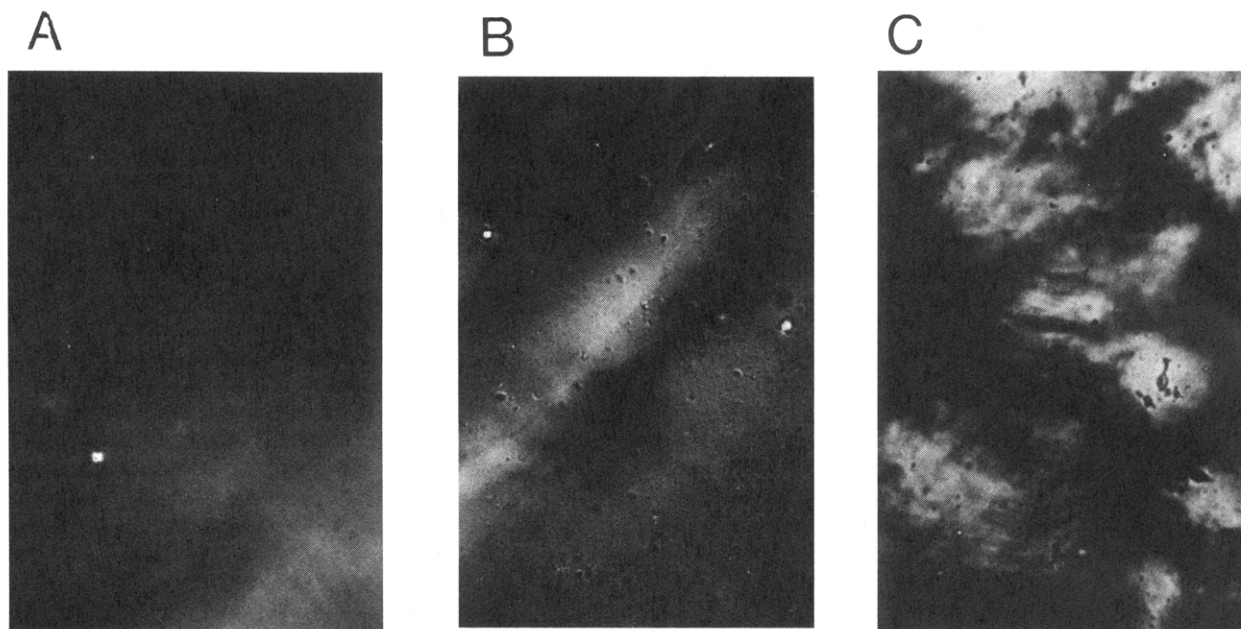


**Figure 4.** Polarized light microscopy of partially anisotropic DNA solutions with different total DNA concentrations. The original magnification was 20 $\times$  for all samples. (a) 14 mg/mL (10% anisotropy); (b) 29 mg/mL (38% anisotropy); (c) 62 mg/mL (98% anisotropy).

(Figure 4B). At 47 mg of DNA/mL (80% anisotropic) the sample showed a high background birefringence along with areas containing "brush stroke"-like textures (Figure 4C). Samples allowed to dry slowly beyond the highest concentrations examined by NMR (not shown) gradually became highly striated and colored with textures reminiscent of, but not identical to, those observed for the columnar phase of shorter DNA fragments.<sup>36,41</sup>

## Discussion

In a recent review, Vroege and Lekkerkerker<sup>42</sup> compared the extensions of Onsager theory to experimental results obtained by various researchers and found reasonable correlation for semiflexible, nonelectrolyte systems such as PHIC in dichloromethane<sup>6</sup> and Schizophyllan in water<sup>43</sup> and for the polyelectrolyte, xanthan, in water.<sup>9,10</sup> The authors remarked on the incomplete characterization of the phase behavior of DNA and indicated that more work needs to be done in the field. The present studies were undertaken to characterize for the first time the phase behavior of very long DNA. This DNA has an average length of about 8 kilobase pairs, corresponding to a contour length  $\approx 2.7 \mu\text{m}$ , a hard-core axial ratio  $\approx 1100$ , or  $N_P \approx 54$  persistence lengths (for  $P = 50 \text{ nm}$ ).

"Solid-state" <sup>31</sup>P NMR spectroscopy provides a means for quantitatively distinguishing between isotropic and anisotropic phases of extraordinarily long DNA in biphasic solutions that do not readily phase separate. (Attempts to separate phases by low-speed centrifugation as described by Teramoto and co-workers<sup>6,10</sup> for other polymers were not successful.) NMR measurements indicated that solutions of long DNA at a Na<sup>+</sup> concentration of 0.1 M become partly anisotropic at  $C_i^* = 13 \text{ mg/mL}$  and fully anisotropic at  $C_a^* = 67 \text{ mg/mL}$ . Positive confirmation of anisotropic phase formation at the lowest concentration by polarized light microscopy was essential since resonance line widths principally monitor dynamics, rather than anisotropy, and small amounts of the anisotropic phase are difficult to detect by NMR.

While the phase transitions of this DNA are qualitatively in accord with expectations, there are substantial quantitative deviations. The DNA critical concentrations can be compared to those observed experimentally for xanthan

and to predictions of recent theoretical treatments of semiflexible polyelectrolytes. In the latter respect we restrict our discussion mainly to the results of Vroege and Odijk,<sup>44,46</sup> who obtained expressions for critical concentrations in the limit of  $L \gg P \gg D_{\text{eff}}$ , where  $L$ ,  $P$ , and  $D_{\text{eff}}$  are the chain contour length, persistence length, and effective diameter, respectively. These conditions are well met for the present DNA. Khoklov and Semenov<sup>3</sup> and Odijk<sup>4</sup> have emphasized that the critical length scale determining anisotropic phase transitions for wormlike semiflexible chains is  $P$ , since  $P$  (and not  $L$ ) is related to the distance  $\lambda \ll P$  required to travel along the anisotropic chain before the chain deflects back to the director. Two other effects must be included for a polyelectrolyte: the increase in chain diameter due to the ion double layer as expressed by  $D_{\text{eff}}$  (which lowers  $C_{i,a}^*$ ) and a twisting effect due to repulsive interactions between two parallel rods expressed by the twist parameter  $h$  (which increases  $C_{i,a}^*$ ). Both  $D_{\text{eff}}$  and  $h$  are dependent on the character of the double layer, treated in terms of the nonlinear Poisson-Boltzmann equation,<sup>45</sup> and hence on the polymer charge density and supporting electrolyte concentration.

According to Vroege,<sup>46</sup> the limiting critical concentrations  $c_i$  and  $c_a$  in dimensionless units are given by

$$c_i = \frac{0.3588}{1 - \sqrt{x}} \quad \text{and} \quad c_a = \frac{0.3588}{x - \sqrt{x}} \quad (2a,b)$$

where  $x = 0.8648 + 0.0091h$ . The dimensionless concentrations are related to the usual concentrations in  $\text{mg/cm}^3$  by

$$C_{i,a}^* = c_{i,a} \left[ \frac{4}{\pi} \left( \frac{1}{D_{\text{eff}} P L} \right) \left( \frac{M}{N_A \nu} \right) \right] \quad (3)$$

Inatomi et al.<sup>10</sup> reported values of  $C_i^* = 39 \text{ mg/mL}$  and  $C_a^* = 51 \text{ mg/mL}$  for their highest molecular weight sample of xanthan ( $M_v = 9.8 \times 10^5$ ,  $L = 505 \text{ nm}$ ,  $N_P = 4.2$ ) in 0.1 M NaCl. Although this chain represents only a few persistence lengths, calculation of the infinite chain limit according to ref 46 would decrease these values only by about 10%. As shown in Table 1, good agreement is obtained between critical concentrations observed for xanthan and the calculated limit values (with physically

**Table 1. Theoretical Limiting Values of the Critical Concentrations  $C_i^*$  and  $C_a^*$  of Xanthan ( $N_p = 4.2$ )<sup>a</sup>**

$D_{\text{eff}}$ (nm)	crit concn $C_i^*$		crit concn $C_a^*$	
	$P =$ 120 nm	$P =$ 240 nm	$P =$ 120 nm	$P =$ 240 nm
4	51.2	25.6	54.2	27.2
4.5	45.5	22.8	48.4	24.2
5	41.0	20.5	43.6	21.8
5.5	37.2	18.6	39.6	19.8
6	34.1	17.1	36.3	18.2

<sup>a</sup> Calculated according to Vroege,<sup>46</sup> for the indicated values of the effective diameter and persistence length and a twist parameter of  $h = 0.191$ .

reasonable values of  $D_{\text{eff}}$  and  $h = 0.191^{46}$ ) only for  $D_{\text{eff}} \approx 5.0$  nm and  $P \approx 120$ , which correspond to the determined values<sup>10</sup> for  $D_{\text{eff}}$  and  $P$ . In this case  $C_i^* = 41$  mg/mL and  $C_a^* = 44$  mg/mL; hence, the predicted width of the biphasic region is somewhat smaller than observed, the larger contradiction being the low predicted value of  $C_a^*$ .

By contrast, the DNA anisotropic phase is observed at a concentration  $C_i^*$  significantly lower than that of xanthan (regardless of the extrapolation method), despite the much smaller DNA persistence length. No physically reasonable combinations of  $D_{\text{eff}}$  and  $h$  come close to duplicating  $C_i^*$  for  $P_{\text{DNA}} = 50$ –100 nm, this range being comprehensive of the maximum estimates of the static persistence length of mixed sequence DNA in dilute solution.<sup>47</sup> (The most recent transient electric dichroism measurements made on discrete length DNA fragments indicate a persistence length in a narrower range of about 45–60 nm and little dependence of the persistence length on ionic strength above 10 mM.<sup>47</sup>) The twisting parameter  $h$  has very modest influences on  $C_{i,a}^*$  and is not considered further. (Values of  $h = 0.10$ – $0.15$  for DNA correspond to supporting electrolyte concentrations spanning from  $\approx 0.01$  to 1 M.) Assumption of  $D_{\text{eff}}$  in a reasonable range of 5–8 nm for 0.1 M  $\text{Na}^+$  requires  $P_{\text{DNA}} \approx 200$ –300 nm to account for  $C_i^*$  as low as 14 mg/mL. On the other hand, the considerably higher concentration required for complete anisotropic phase formation,  $C_a^* = 67$  mg/mL, is consistent with a DNA persistence length in the expected range of  $P_{\text{DNA}} = 50$ –100 nm.

The major inconsistency between the expected and observed anisotropic phase formation of very long DNA is thus the ready onset of anisotropy and the consequent extreme broadening of the biphasic region. The breadth of the biphasic region suggests a 5-fold difference in the DNA concentrations of the isotropic and anisotropic phases ( $C_a^*/C_i^* = 5.1$ ), much larger than that observed for other noninteracting semirigid polymers. While length heterogeneity broadens the biphasic region for mixtures of shorter polymer lengths, the extremity of lengths represented here, with virtually all molecules being many times the persistence length (80% with  $N_p \geq 27$  and  $\approx 100\%$  with  $N_p > 7$ ), mitigates against this simple explanation. An unexpectedly low critical concentration ( $C_i^*$ ) for the appearance of the anisotropic phase could result from weak attractive interactions between DNA molecules. However, if there are weak, uniformly distributed interactions between long DNA molecules, then the good agreement between the observed  $C_a^*$  and that predicted for DNA with a persistence length of 50 nm is difficult to explain. Both theory and experimental precedents show that attractive interactions between long, semirigid polymers affect  $C_a^*$  more strongly than  $C_i^*$ ; that is, broadening of the biphasic region results more from an increase in  $C_a^*$  than a decrease in  $C_i^*$  (see, for example, refs 48 and 49).

**Table 2. Theoretical Limiting Values of the Critical Concentrations  $C_i^*$  and  $C_a^*$  of Very Large DNA<sup>a</sup>**

$D_{\text{eff}}$ (nm)	crit concn $C_i^*$				
	$P =$ 50 nm	$P =$ 100 nm	$P =$ 150 nm	$P =$ 200 nm	$P =$ 250 nm
4	119	59.7	39.8	29.8	23.9
5	95.5	47.8	31.8	23.9	19.1
6	79.6	39.8	26.5	19.9	15.9
7	68.2	34.1	22.7	17.1	13.6
8	59.7	29.8	19.9	14.9	11.9
9	53.1	26.5	17.7	13.3	10.6
10	47.5	23.9	15.9	11.9	9.6

$D_{\text{eff}}$ (nm)	crit concn $C_a^*$				
	$P =$ 50 nm	$P =$ 100 nm	$P =$ 150 nm	$P =$ 200 nm	$P =$ 250 nm
4	127	63.6	42.4	31.8	25.5
5	111	50.9	33.9	25.4	20.4
6	84.9	42.4	28.3	21.2	17.0
7	72.7	36.4	24.2	18.2	14.6
8	63.6	31.8	21.2	15.9	12.7
9	56.6	28.2	18.9	14.1	10.6
10	50.9	25.5	17.0	12.7	9.6

<sup>a</sup> Calculated according to Vroege,<sup>46</sup> for the indicated values of the effective diameter and persistence length and a twist parameter of  $h = 0.15$ .

Alternatively, there may be fundamental features of DNA not addressed in the theory. It is premature to pursue this question in detail without greater knowledge of the length dependencies of the critical concentrations (experiments in progress). There may be merit, however, in pointing out features of DNA not provided for in the theory or present in simple repeat polymers. Though still speculative on certain points, the concepts that the local flexibility and intrinsic curvature of DNA vary with base sequence are gaining acceptance.<sup>47,50–54</sup> Since the dominant length scale for extremely long DNA is the persistence length, not the contour length, segmental variations in  $P$  are expected to strongly influence the ordering behavior. Recent studies using spectroscopic techniques that monitor internal dynamics have indicated that the dynamic flexural persistence length of DNA is significantly greater than the static persistence length. Estimates of the dynamic persistence length are in the range from 150 to 280 nm,<sup>55–58</sup> close to values required to predict the observed  $C_i^*$ , but not  $C_a^*$ . At present it is unclear whether the dynamic persistence length is more important than the static persistence length in determining the self-ordering properties of semirigid polymers, whether a discrepancy between static and dynamic persistence lengths is unique to DNA, or whether the dynamic persistence length is DNA sequence-dependent.

As observed for shorter DNA, this very long DNA seems capable of forming more than one ordered phase. The failure of these phases to form well-developed, microscopically distinct, textures can be rationalized in terms of the extreme lengths of individual molecules preventing formation of well-defined defects between distinguishable microdomains. Phase separation and defect development would be further suppressed if variations in flexibility along the chain cause preferential segregation of the most rigid chain segments into the anisotropic phase. Technical difficulties in preparing thin specimens of these extraordinarily viscous samples also contribute to the lack of detail. For example, distinguishable, but poorly developed cholesteric fringe patterns have been observed near the liquid edges in a few specimens (not shown). More extensive microscopic studies will be described elsewhere.

It is evident from these results that very large DNA forms anisotropic phases at modest concentrations well in

the physiological range. The ready ability of long DNA to self-order is consistent with various models that describe as liquid crystalline the packing of DNA in several natural settings such as bacterial nucleoids, dinoflagellate chromosomes, sperm heads, and virus capsids.<sup>59,60</sup> The possibility that segmental variations in chain flexibility may influence the self-ordering properties of DNA is intriguing and could also have biological significance.

## References and Notes

- (1) Onsager, L. *Ann. N.Y. Acad. Sci.* **1949**, *51*, 627.
- (2) Stroobants, A.; Lekkerkerker, H. N. W.; Odijk, Th. *Macromolecules* **1986**, *19*, 2232.
- (3) Khokhlov, A. R.; Semenov, A. N. *Physica A (Amsterdam)* **1981**, *108A*, 546.
- (4) Odijk, Th. *Macromolecules* **1986**, *19*, 2313.
- (5) Conio, C.; Bianchi, E.; Ciferri, A.; Krigbaum, W. R. *Macromolecules* **1984**, *17*, 856.
- (6) Itou, T.; Teramoto, A. *Macromolecules* **1988**, *21*, 2225.
- (7) Miller, W. *Annu. Rev. Phys. Chem.* **1979**, *29*, 219.
- (8) Itou, T.; Sato, T.; Teramoto, A.; Aharoni, S. M. *Polym. J.* **1988**, *20*, 1049.
- (9) Sato, T.; Kakihara, T.; Teramoto, A. *Polymer* **1990**, *31*, 824.
- (10) Inatomi, S.; Jinbo, Y.; Sato, T.; Teramoto, A. *Macromolecules* **1992**, *25*, 5013.
- (11) Robinson, C. *Tetrahedron* **1961**, *13*, 219.
- (12) Brian, A. A.; Frisch, H. L.; Lerman, L. S. *Biopolymers* **1981**, *20*, 1305.
- (13) Luzzati, V.; Nicolaieff, A.; Masson, F. *J. Mol. Biol.* **1961**, *3*, 185.
- (14) Bouligand, Y. *Tissue Cell* **1972**, *4*, 189.
- (15) Livolant, F.; Bouligand, Y. *J. Phys. (Paris)* **1986**, *47*, 1813.
- (16) Livolant, F. *J. Phys. (Paris)* **1987**, *48*, 1051.
- (17) Livolant, F.; Bouligand, Y. *Chromosoma* **1978**, *68*, 21.
- (18) Lerman, L. S. *Cold Spring Harbor Symp. Quant. Biol.* **1974**, *38*, 59.
- (19) Lerman, L. S. *Proc. Natl. Acad. Sci. U.S.A.* **1971**, *68*, 1886.
- (20) Jordan, C. F.; Lerman, L. S.; Venable, J. H. *Nature (New Biol.)* **1972**, *236*, 67.
- (21) Maniatis, T.; Venable, J. H., Jr.; Lerman, L. S. *J. Mol. Biol.* **1974**, *84*, 37.
- (22) Iizuka, E. *Polym. J.* **1977**, *9*, 173.
- (23) Iizuka, E. *Polym. J.* **1978**, *10*, 237.
- (24) Iizuka, E. *Polym. J.* **1978**, *10*, 293.
- (25) Iizuka, E.; Kondo, Y. *Mol. Cryst. Liq. Cryst.* **1979**, *51*, 285.
- (26) Maret, G.; Dransfeld, K. *Physica* **1977**, *86-88B*, 1077.
- (27) Maret, G.; Dransfeld, K. In *Topics in Applied Physics*; Herlach, F., Ed.; Springer-Verlag: New York, 1985; pp 143-204.
- (28) Maret, G.; Schickfus, M.; Mayer, A.; Dransfeld, K. *Phys. Rev. Lett.* **1975**, *35*, 397.
- (29) Senechal, E.; Maret, G.; Dransfeld, K. *Int. J. Biol. Macromol.* **1980**, *2*, 256.
- (30) Brandes, R.; Kearns, D. R. *Biochemistry* **1986**, *25*, 5890.
- (31) Rill, R. L.; Hilliard, P. R., Jr.; Levy, G. C. *J. Biol. Chem.* **1983**, *258*, 250.
- (32) Rill, R. L. *Proc. Natl. Acad. Sci. U.S.A.* **1985**.
- (33) Strzelecka, T. E.; Rill, R. L. *J. Am. Chem. Soc.* **1987**, *109*, 4513.
- (34) Strzelecka, T. E.; Rill, R. L. *Biopolymers* **1990**, *30*, 57.
- (35) Strzelecka, T. E.; Rill, R. L. *Biopolymers* **1990**, *30*, 803.
- (36) Strzelecka, T. E.; Davidson, M. W.; Rill, R. L. *Nature* **1988**, *331*, 457.
- (37) Lis, J. T. Fractionation of DNA Fragments by Polyethylene Glycol Induced Precipitation. *Methods in Enzymology*; 1980; Vol. 65, pp 347-353.
- (38) Strzelecka, T. E. Liquid crystalline phases in concentrated DNA solutions. Ph.D. Dissertation, University Microfilms, 1989.
- (39) Glantz, S. A.; Slinker, B. K. *Primer of Applied Regression and Analysis of Variance*; McGraw-Hill, Inc.: New York, 1990.
- (40) Rill, R. L.; Strzelecka, T. E.; Davidson, M. W.; Van Winkle, D. H. *Physica A* **1991**, *176*, 87.
- (41) Livolant, F.; Levelut, A. M.; Doucet, J.; Benoit, J. P. *Nature* **1989**, *339*, 724.
- (42) Vroege, G. J.; Lekkerkerker, H. N. W. *Rep. Prog. Phys.* **1992**, *55*, 1241.
- (43) Kojima, T.; Itou, T.; Teramoto, A. *Polym. J.* **1987**, *19*, 1225.
- (44) Vroege, G. J.; Odijk, T. *Macromolecules* **1988**, *21*, 2848.
- (45) Philip, J. R.; Wooding, R. A. *J. Chem. Phys.* **1970**, *52*, 953.
- (46) Vroege, G. J. *J. Chem. Phys.* **1989**, *90*, 4560.
- (47) Hagerman, P. J. *Annu. Rev. Biophys. Biophys. Chem.* **1988**, *17*, 265.
- (48) Ciferri, A. Phase Behavior of Rigid and Semirigid Mesogens. In *Liquid Crystallinity in Polymers: Principles and Fundamental Properties*; Ciferri, A., Ed.; VCH: New York, 1991; pp 209-259.
- (49) Ciferri, A. *Liquid Crystallinity in Polymers: Principles and Fundamental Properties*; VCH: New York, 1991.
- (50) Trifonov, E. *CRC Crit. Rev. Biochem.* **1985**, *19*, 89.
- (51) Maroun, R. C.; Olson, W. K. *Biopolymers* **1988**, *27*, 561, 585.
- (52) Nadeau, J. G.; Crothers, D. M. *Proc. Natl. Acad. Sci. U.S.A.* **1989**, *86*, 262.
- (53) Sarai, A.; Mazur, J.; Nussinov, R.; Jernigan, R. L. *Biochemistry* **1989**, *28*, 7842.
- (54) Taylor, W. H.; Hagerman, P. J. *J. Mol. Biol.* **1990**, *212*, 363.
- (55) Porschke, D. *Biophys. Chem.* **1991**, *40*, 169.
- (56) Song, L.; Schurr, J. M. *Biopolymers* **1990**, *30*, 229.
- (57) Schurr, J. M.; Fujimoto, B. S.; Wu, P.; Song, L. In *Topics in Fluorescence Spectroscopy, Vol. 3: Biological Applications*; Lakowicz, J. R., Ed.; Plenum Press: New York, 1992.
- (58) Hustedt, E. J.; Spaltenstein, A.; Kirchner, J. J.; Hopkins, P. B.; Robinson, B. H. *Biochemistry* **1993**, *32*, 1774.
- (59) Lepault, J.; Dubochet, J.; Baschong, W.; Kellenberger, E. *EMBO J.* **1986**, *6*, 1507.
- (60) Booy, F. P.; Newcomb, W. W.; Trus, B. L.; Brown, J. C.; Baker, T. S.; Steven, A. C. *Cell* **1991**, *64*, 1007.